

Structure and organization in inclusion-containing bilayer membranes

Chun-Lai Ren and Yu-qiang Ma*

*National Laboratory of Solid State Microstructures,
Nanjing University, Nanjing 210093, China*

Abstract

Based on a considerable amount of experimental evidence for generic properties of lateral organization of lipid membranes containing inclusions, we first present a general model system of bilayer membranes embedded by nanosized inclusions, and account well for a series of unexpected behaviors in related experimental findings. (1) The appearance and disappearance of lipid/inclusion-rich rafts are observed with increasing the inclusion content. (2) The chain arrays of inclusions may form at high concentrations. (3) Location of inclusions changes with increasing the inclusion content, and may undergo a layering transition from one-layer located in the center of the bilayer to two-layer structure arranged in opposing leaflets of a bilayer. (4) The membrane fluidity is enhanced by the presence of inclusions. Our theoretical predictions address the complex interactions between membranes and inclusions, suggesting a unifying mechanism which reflects the competition between the conformational entropy of lipids favoring the formation of lipid-rich rafts and the steric repulsion of inclusions leading to the uniform dispersion. The present study advances our understanding of membrane organization by unifying these experimental evidences of real biomembranes with inclusions which can be different, but with the hydrophobic and rigid properties.

PACS numbers: 87.16.Dg, 87.14.Cc, 87.68.+z, 64.75.+g

*Corresponding author: myqiang@nju.edu.cn

Recently, there is growing evidence that due to the presence of inclusions within membranes, the distribution of lipids is inhomogeneous, where lateral segregation could induce the formation of lipid/inclusion-rich raft domains. For instance, cholesterol which is one of the most important regulators of lipid organization, prefers to have conformationally ordered lipid chains next to it due to its hydrophobically smooth and stiff steroid ring structure[1, 2], and promotes the formation of lipid rafts(see, for example, reviews[1, 3, 4] and recent research works[5]). On the other hand, it was reported [6] that hydrophobic drugs such as taxol(paclitaxel)[6, 7] and dipyridamole(DIP)[8]) may assist the formation of lipid/drug-enriched raft domains, and increase with increasing the drug content, but disappear at high concentrations, which has also been observed in cholesterol-lipid systems [9]. Particularly, the perturbed lipids may lead to chaining of cholesterol [9, 10] or drugs [6, 11] inside the bilayer. Furthermore, the introducing of taxol drug into the lipid layer will perturb the hydrocarbon chain conformation, which may increase membrane fluidity[6, 7, 11]. Most recently, some foreign inclusions such as silver nanoparticles were reported to have similar effects on the membrane fluidity[12].

Despite the common properties of membrane organization due to distinct inclusions and despite its important significance in cellular functions such as signal transduction and membrane trafficking[3], the influence of the inclusions on such a change in lateral organization has not yet been considered in computational and theoretical investigations, and further insight into the mechanisms behind general evidence from lipid-inclusion complexes remains poor[13]. Previous theoretical works were concerned with the hydrophobic mismatch interaction between inclusions[14, 15, 16] and the possible formation of lipid rafts[1, 13]. However, a detailed structural change with varying the inclusion content has not been systematically elucidated. In this letter, we examine a simple model that not only allows us to present a unifying description of these phenomena with varying inclusion concentrations, but also sheds light on physical mechanism behind membrane organization due to distinct inclusions such as intrinsic membrane protein, cholesterol, hydrophobic drug, or other bionanoparticles.

Consider a lipid bilayer membrane containing n_d inclusions of radius R in an aqueous environment(Fig. 1). The volume of system is $V = L_x \times L_y \times L_z$, where L_x and L_y are lateral membrane lengths under periodical boundary conditions, and L_z is the size of system along the membrane normal direction. The bilayer membrane is composed of one type of lipids with two hydrophobic tails. The number of lipids is given by $n_l = 2 \times$

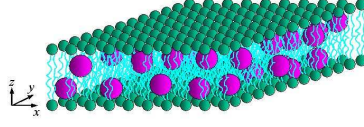


FIG. 1: (color) A schematic of the lipid bilayer membrane containing inclusions.

$\sigma \times L_x \times L_y$, where σ is the number density of lipids in one leaflet. The headgroup of lipids has the volume v_h , and two equal-length tails composed of $N/2$ segments each are assumed as flexible Gaussian chains[17]. The segment has the volume ρ_0^{-1} and the length a . Thanks to the smooth and rigid property of bioinclusions compared with the flexible lipids[1, 4, 14], we assume inclusions as hard-sphere nanoparticles. The concentrations of the head and tails of lipids are $\phi_h = n_l v_h / V$ and $\phi_t = n_l N \rho_0^{-1} / V$, and the inclusions $\phi_d = 4\pi R^3 n_d / 3V$. The solvent molecules have the volume v_s and the concentration $\phi_s = 1 - \phi_t - \phi_h - \phi_d$ [18]. Recently, the self-consistent field theory (SCFT) has been proven to be powerful in calculating equilibrium morphologies in polymeric systems[19, 20, 21], while nanoparticles can be treated by density-functional theory (DFT) [22] to account for steric packing effects of particles. Interestingly, Thompson et al. [19] developed a hybrid SCFT/DFT approach to study mixtures of diblock copolymer and nanoparticles. On the other hand, the SCFT method is extended to successfully study the phase behavior of pure lipid systems[13, 17, 23]. Here, we will extend the hybrid SCFT/DFT approach[19] to calculate the structural organization of the bilayer membrane in the presence of inclusions. The resulting free energy F for the present system [24] is given by

$$\begin{aligned}
\frac{NF}{\rho_0 k_B T V} = & -\phi_t \ln\left(\frac{Q_t}{V\phi_t}\right) - \frac{\phi_s}{\alpha_s} \ln\left(\frac{Q_s}{V\phi_s}\right) - \frac{\phi_d}{\alpha} \ln\left(\frac{Q_d \alpha}{V\phi_d}\right) \\
& + \frac{1}{V} \int d\mathbf{r} [\chi_{th} N \varphi_t(\mathbf{r}) \varphi_h(\mathbf{r}) + \chi_{ts} N \varphi_t(\mathbf{r}) \varphi_s(\mathbf{r}) \\
& + \chi_{td} N \varphi_t(\mathbf{r}) \varphi_d(\mathbf{r}) + \chi_{hs} N \varphi_h(\mathbf{r}) \varphi_s(\mathbf{r}) \\
& + \chi_{hd} N \varphi_h(\mathbf{r}) \varphi_d(\mathbf{r}) + \chi_{sd} N \varphi_s(\mathbf{r}) \varphi_d(\mathbf{r}) \\
& - w_t(\mathbf{r}) \varphi_t(\mathbf{r}) - w_h(\mathbf{r}) \varphi_h(\mathbf{r}) - w_s(\mathbf{r}) \varphi_s(\mathbf{r}) \\
& - w_d(\mathbf{r}) \varphi_d(\mathbf{r}) - \xi(\mathbf{r}) (1 - \varphi_t(\mathbf{r}) - \varphi_h(\mathbf{r}) \\
& - \varphi_s(\mathbf{r}) - \varphi_d(\mathbf{r})) + \rho_d(\mathbf{r}) \Psi_{hs}(\overline{\varphi}_d)] , \tag{1}
\end{aligned}$$

where $\alpha_s = v_s \rho_0 / N$, and $\alpha = 4\pi R^3 \rho_0 / 3N$. χ_{th} , χ_{ts} , χ_{td} , χ_{hs} , χ_{hd} , and χ_{sd} are the Flory interaction parameters between tail-head, tail-solvent, tail-inclusion, head-solvent, head-inclusion, and solvent-inclusion, respectively. $\varphi_t(\mathbf{r})$, $\varphi_h(\mathbf{r})$, $\varphi_d(\mathbf{r})$, and $\varphi_s(\mathbf{r})$ are the local

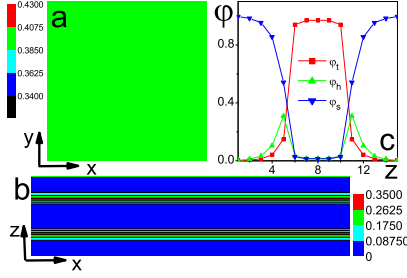


FIG. 2: (color) The pure bilayer membrane in an aqueous environment. (a) The top view of averaged density distribution of lipid tails in the upper leaflet. (b) laterally averaged density profiles of solvent(ϕ_s), lipid tail(ϕ_t), and head group(ϕ_h) along z axes. (c) The x - z cross-section of density distribution of lipid heads averaged in the y -direction.

volume fractions of lipid tail, head group, inclusion, and solvent, and $w_t(\mathbf{r})$, $w_h(\mathbf{r})$, $w_d(\mathbf{r})$, and $w_s(\mathbf{r})$ are corresponding self-consistent fields. $\xi(\mathbf{r})$ ensures the incompressibility of the system, and $\rho_d(\mathbf{r})$ stands for the inclusion center distribution. Q_l , Q_s , and Q_d are respective partition functions for lipid, solvent, and inclusions[19]. The last term in Eq. (1) is the nonideal steric interaction term [22] with the weighted inclusion density $\bar{\varphi}_d(\mathbf{r})$ [19]. The fields and densities are then determined by minimizing the free energy in Eq.(1), and the resulting self-consistent equations can be solved numerically[19]. To reasonably describe the interactions of hydrophobic inclusions dispersed in bilayer lipids with hydrophilic heads and hydrophobic tails, we choose $\chi_{hs}N = 0$, $\chi_{td}N = 3.5$, $\chi_{hd}N = 15.0$, $\chi_{ts}N = 15.0$, $\chi_{sd}N = 20.0$, and $\chi_{th}N = 25.0$. The other parameters are fixed to be $N = 30$, $v_h = v_s = 6\rho_0^{-1}$, $\sigma = 0.08$, $L_x = L_y = 60a$, and $L_z = 15a$. Here, the chosen L_z was large enough, ensuring the solvent concentration $\phi_s = 1$ at $z = 0$ and L_z .

We first examine the case of a bilayer membrane in an aqueous environment in the absence of inclusions. Figure 2a shows the lateral distribution of lipid tails in one leaflet, which is uniform. The distribution is symmetrical with respect to the opposing leaflet. Figure 2b provides the average distribution of headgroups in the x - z cross-sections, reflecting that the shape of membrane surfaces is smooth in the absence of inclusions, since the lipid length is matched. In this case, the membrane is in a gel phase for the limited lateral mobility[9, 11], where lipid tails tightly pack and hardly move in the pure membrane. Figure 2c shows the laterally averaged density profiles of ϕ_t , ϕ_h , and ϕ_s across a bilayer, which displays the

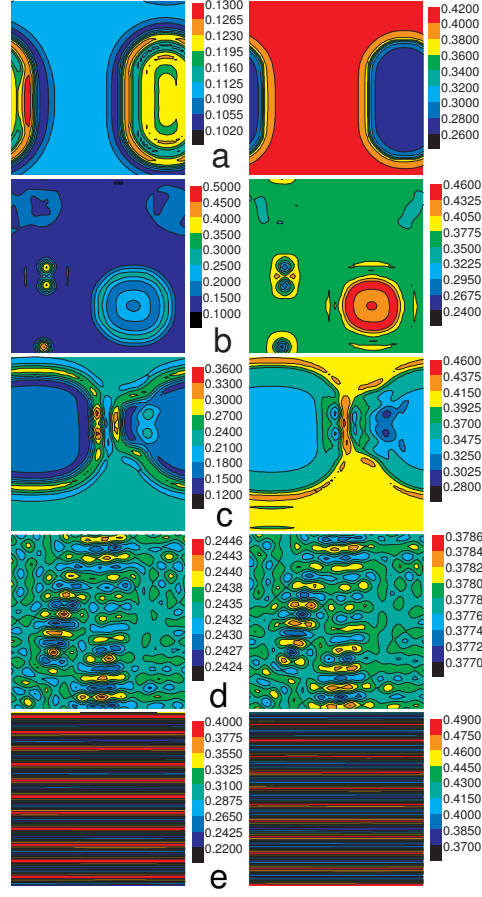


FIG. 3: (color) The top views of averaged density distributions of inclusions (left) and lipid tails (right) in upper leaflet. (a) $\phi_d = 0.10$, (b) $\phi_d = 0.15$, (c) $\phi_d = 0.20$, (d) $\phi_d = 0.24$, and (e) $\phi_d = 0.32$. Here we fix $R = 2.5a$ which is smaller than the membrane thickness.

basic structure of the bilayer and is favorably comparable with mesoscopic simulation and other coarse-grained models describing the bilayer composition[23, 25]. This validates the used SCFT which can reasonably explore conformational properties of lipids, in contrast to phenomenological models that ignore much of the internal structure of the bilayer[13]. Particularly, the approach will become powerful in exploring the lateral inhomogeneity of membrane with inclusions, in contrast to other field theory or simulation schemes[13], where the only one-dimensional density profiles along the membrane normal is shown in the cost of including molecular details of lipids.

Figure 3 shows the in-plane density distributions of inclusions in the left column and the lipid tails in the right column with increasing the inclusion concentration ϕ_d . When ϕ_d is low,

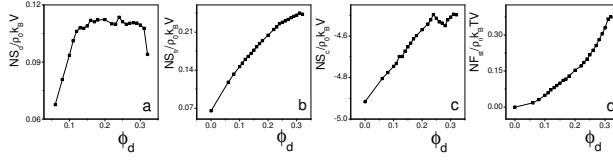


FIG. 4: (a) The translational entropy S_d of inclusions, (b) The translational entropy S_{tr} of lipids, (c) the conformational entropy S_c of lipids, and (d) the steric energy F_{st} of inclusions vs the inclusion concentration.

the translational entropy of inclusions has a significant contribution to the free energy of the system. Any compositional fluctuation of inclusions may lead to the lateral inhomogeneity of lipid composition, in which lipids are depleted in the inclusion-rich regions for ensuring the large translational entropy of inclusions (Fig. 3a). Astonishingly, as ϕ_d is increased, the lipid/inclusion-rich rafts appear (Fig. 3b). In this case, the entropic contribution of lipids becomes significant, and tail chains closing to the rigid surfaces of inclusions can get extra conformational flexibility [1, 12, 16, 26], which enriches the lipids surrounding inclusions. Therefore, inclusions are accumulated in certain membrane regions, which leads to the formation of lipid-rich rafts. The raft size may be enlarged by increasing ϕ_d (Fig. 3c). Interestingly, as ϕ_d is added to a certain range ($\phi_d = 0.24 \sim 0.28$), lipid-rich rafts disappear, but instead the uniform distribution of both inclusion and lipid tail occurs (Fig. 3d). This unexpected behavior provides a strong support for the experimental findings in drug-membrane [6] and cholesterol-membrane [9] complexes. This is due to the strong steric repulsion from large numbers of inclusions, which leads to the uniform dispersion of inclusions. Further increase of ϕ_d leads to the deformation of lipids which produces the effective attraction between inclusions. The deformed conformational entropy can partially be released by chaining of inclusions under the lipid-mediated attraction, shown in Fig. 3e. Such a regularly modulated inclusion-rich stripe structure has been reported in the drug-membrane [6, 11] and cholesterol-membrane complexes [9, 10] where the lipids form ribbons between the aligned cholesterol domains.

Figure 4a shows the translational entropy S_d of inclusions. For low ϕ_d , the large increase of S_d with ϕ_d indicates that S_d plays an important role at first, which can account well for the formation of the weak inhomogeneous distribution of lipids (Fig. 3a) to ensure large translational entropy of inclusions. For large ϕ_d , S_d decreases with the appearance of the

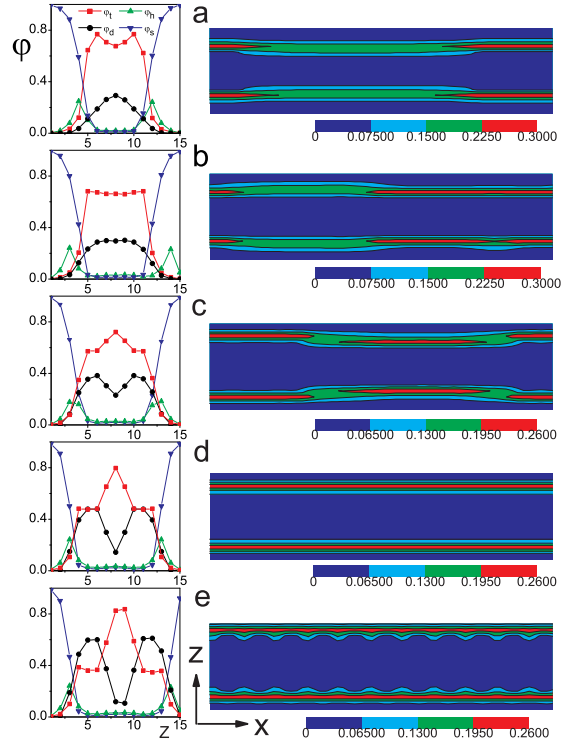


FIG. 5: (color) Laterally averaged density profiles of solvent(φ_s), lipid tail(φ_t), head group(φ_h), and inclusion (φ_d) along z axes (left), and the x - z cross-sections of density distributions of lipid heads averaged in the y -direction(right). Parameters are the same in Fig. 2.

chaining structure. Figure 4b shows the translational entropy S_{tr} of lipids. The curve goes up monotonously, meaning that the addition of inclusions increases the lateral membrane fluidity, which is a characteristic of gel-liquid transition[9, 11]. The reason is that lipid tails are stretched along the bilayer normal, which increases translational degrees of freedom and thus enhances the lateral mobility of lipids[1]. Figure 4c shows the conformational entropy S_c of lipids. Beginning from a low conformational entropy in the gel phase of the pure membrane, lipids get more conformations with the perturbation of added inclusions where the lipid-enriched rafts are formed. However, there is a small decrease in the range $\phi_d = 0.24 \sim 0.28$ with the disappearance of lipid rafts, where all lipids are strongly stretched with the same length. Figure 4d shows the steric repulsion energy F_{st} of inclusions, which increases with increasing ϕ_d . Therefore, it is the steric repulsion between inclusions that suppresses lipid rafts. For high ϕ_d , the repulsion of inclusions is stronger, but at the same time, the deformed lipid-mediated attraction between inclusions becomes also stronger. The

only way that the conformational entropy of deformed lipids is released(Fig. 4c), is to drive inclusions to assemble anisotropically along one direction. As a result, the deformed lipids provide an additional lateral anisotropic interaction between inclusions, which stabilizes the parallel chain arrays of inclusions.

Finally, Fig. 5 shows laterally averaged density profiles of different components across the bilayer in the left column and average density distributions of lipid heads in x-z cross-sections in the right column. For low ϕ_d (Fig. 5a), the inclusions assemble in the bilayer midplane for the membrane stability, which is displayed by one peak of density profiles (φ_d) of inclusions. With increasing ϕ_d , one peak density profile may be saturated (Fig. 5b), and further increase of inclusions leads to the occurrence of two peaks of φ_d (Fig.5c-e), implying the relocation of inclusions where the two-layer distribution of inclusions is arranged in opposing leaflets of a bilayer[26]. Previous experiment[11] on drug-membrane complexes has also shown that the location of drugs in the bilayer depends on drug content. The two-layer distribution of inclusions ensures that the ends of lipid tails can still remain in the membrane midplane favoring the conformation of lipids. On the other hand, in Fig. 5a-c, the irregular density distribution of headgroups originates from the lipid chain-length mismatch, while in Fig. 5d, the membrane surfaces become flat with a matched length of strongly stretched lipids where lipid-rich domains disappear. By comparison of the distances between two peaks of head profiles (φ_h) in the left side of Fig. 5, we also find that the thickness of membrane continuously increases with the addition of inclusions.

This work was supported by the National Natural Science Foundation of China, Nos. 10334020, 20674037, and 10574061.

-
- [1] O. G. Mouritsen, *Life - as a matter of fat* (Springer-Verlag, Berlin, 2005).
 - [2] L. Miao et al., *Biophys. J.* **82**, 1429(2002).
 - [3] F. Maxfield and I. Tabas, *Nature* **438**, 612(2005); K. Simons and W. Vaz, *Annu. Rev. Biophys. Biomol. Struct.* **33**, 269(2004); H. McConnell and M. Vrljic, *ibid* **32**, 469(2003); M. Edidin, *ibid* **32**, 257(2003); D. Brown and E. London, *Annu. Rev. Cell Dev. Biol.* **14**, 111(1998).
 - [4] H. Ohvo-Rekila, et al., *Prog. Lipid Res.* **41**, 66(2002).
 - [5] K. Simons and E. Ikonen, *Science* **290**, 1721(2000); T. Baumgart, S. Hess, and W. Webb,

- Nature*, **425**, 821(2003); S. Komura, et al. *Europhys. Lett.* **67**, 011910(2003); H. McConnell and A. Radhakrishnan, *Proc. Natl. Acad. Sci. USA* **103**, 1184(2006); R. Elliott, I. Szleifer, and M. Schick, *Phys. Rev. Lett.* **96**, 098101(2006); S. Veatch and S. Keller, *ibid* **94**, 148101(2005).
- [6] S. Feng, K. Gong, and J. Chew, *Langmuir* **18**, 4061(2002).
- [7] C. Bernsdorff, R. Reszka, and R. J. Winter, *J. Biomed. Mater. Res.* **46**, 141(1999).
- [8] P. Nassar, L. Almeida, and M. Tabak, *Biochim. Biophys. Acta* **1328**, 140(1997); *Langmuir* **14**, 6811(1998).
- [9] J. C. Lawrence et al., *Biophys. J.* **84**, 1827(2003).
- [10] J. Rogers, A. G. Lee, and D. D. Wilton, *Biochim. Biophys. Acta* **552**, 23(1979).
- [11] S. V. Balasubramanian and R. M. Straubinger, *Biochemistry* **33**, 8941(1994).
- [12] S. H. Park et al., *Colloids Surf. B: Biointerfaces* **44**, 117(2005).
- [13] M. Müller, K. Katsov, and M. Schick, *Phys. Rep.*, **434**, 113(2006), and references therein.
- This review has justified the recent applications of coarse-grained SCFT with Gaussian chain model to bilayer membrane.
- [14] M. Venturoli, et al. *Phys. Rep.* **437**, 1(2006).
- [15] M. Sperotto, S. May, and A. Baumgaertner, *Chemistry and Physics of Lipids* **141**, 2(2006); N. Dan, P. Pincus, and S. Safran *Langmuir* **9**, 2768(1993).
- [16] R. Bruinsma and P. Pincus, *Curr. Opin. Sol. St. Mater. Sci.* **1**, 401(1996); S. May, *Langmuir* **18**, 6356(2002).
- [17] X. J. Li and M. Schick, *Biophys. J.* **78**, 34(2000) compares the SCFT results of the lipid system with the experimental results, and a good agreement is found between them, while the real lipid is not completely flexible.
- [18] R. Elliott et al., *J. Chem. Phys.* **122**, 044904-1(2005).
- [19] R. B. Thompson et al., *Science* **292**, 2469(2001); *Macromolecules* **35**, 1560(2002).
- [20] M. W. Matsen and M. Schick, *Phys. Rev. Lett.* **72**, 2660(1994); F. Drolet and G. H. Fredrickson, *ibid* **83**, 4317(1999); C. Ren and Y. Ma, *J. Am. Chem. Soc.* **128**, 2733(2006).
- [21] F. Schmid, *J. Phys.:Condens. Matter* **10**, 8105(1998); G. H. Fredrickson, *The equilibrium theory of inhomogeneous polymers* (Oxford University Press, Oxford, 2006); M. W. Matsen, in *Soft Matter*, eds. G. Gompper and M. Schick (Wiley-VCH, Weinheim, 2006), Volume 1.
- [22] P. Tarazona, *Mol. Phys.* **52**, 81(1984); N. F. Carnahan and K. E. Starling, *J. Chem. Phys.* **51**, 635(1969).

- [23] R. A. Kik, F. A. M. Leermakers, and J. M. Kleijn, *Phys. Chem. Chem. Phys.*, **7**, 19969(2005).
- [24] see Ref.[21] for technical details of the SCFT approach.
- [25] A. L. Frischknecht and L. J. D. Frink, *Phys. Rev. E* **72**, 041924-1(2005); J. C. Shillcock and R. Lipowsky, *J. Chem. Phys.* **117**, 5048(2002).
- [26] M. B. Sankaram and T. E. Thompson, *Biochemistry*, **29**, 10676(1990).